Published by AIT
the Italian Society of Remote Sensing

# Production of DTM quality by TLS data

**Domenica Costantino[1*] and Maria Giuseppa Angelini[2]**

[1]DICAR, Politecnico di Bari, Via Orabona 4, 70125 Bari, Italy
[2]DICATECh, Politecnico di Bari, Via Orabona 4, 70125 Bari, Italy
*Corresponding author, e-mail address: d.costantino@poliba.it

## Abstract
A procedure of calculation and experimentation addressed to a DTM extraction by TLS data has been implemented. The validation of elevation values has been realized by integrating the data collected with classical topographical and GPS observations. The results obtained allowed the assessment of the appropriate and simplified procedure for the determination of the DTM using laser technology and the possibility to improve and verify the attainable accuracy of the altitude plane.
The experimental outputs have been compared with those produced by commercial software. The difference obtained is primarily concerned with the conceptual scheme applied in the definition of the grid in the algorithm of interpolation and obtainable accuracy. Moreover, after obtaining the grid by topographic survey, characterized by a high precision, it is possible to verify its accuracy.
**Keywords:** TLS, DTM, least squares estimation, interpolation.

## Introduction
The construction of a digital elevation model is divided into three main phases: data collection or acquisition of data as (*x, y, z*) into a determined reference system, according to the topology or structure definition of the area, and by interpolation of data in areas where there are no values. The original points are usually spaced irregularly and this depends on the technique used for measurements. The data acquisition can be done using different methods: airborne and terrestrial laser scanner, by digitized contour lines on topographic maps, by terrestrial or aerial photogrammetry and satellite images, by GPS or topographic survey.
Data processing is made by the construction of a digital model, which allows the description of the object along with topological and morphological elements typical of the area investigated. The general approach involves the determination of an analytic function that represents the surface of the object in the form $z = f(x, y)$, where $z$ indicates the share of each point of planimetric coordinates $(x, y)$. So it possible to determine the function $z = f(x, y)$ for any point inside the surface portion to be modeled. The elements that allow the assessment of this function

are acquired points, i.e. triplets of *XYZ* coordinates that define each point on the ground.
The construction of a digital model can be performed with local interpolating procedures, based on the finite element method [Wack and Stelzl, 2005], such as: matrix method (GRID), the interpolation is done with bilinear or bicubic spline functions of dots arranged in the mesh of a regular grid; method of triangulation (TIN, Triangulated Irregular Network), the interpolation is achieved by construction of flat triangles on the original points, in such a way as to form triangles that do not intersect. Both have characteristic features and strengths. GRID in the original set of points, irregularly distributed, is transformed into a regular grid (square mesh equal), using spatial interpolation techniques (i.e. kriging). In the resulting DEM/DSM (Digital Elevation Model/Digital Surface Model), each triplet (*x, y, z*) represents an interpolated square grid also called cell. The main advantages are: the simplicity of the organization of the data that facilitates treatment using a computer and the management of information through a database; the high structural simplicity and topological model; the possibility to compare and evaluate the digital models of the same portion of territory. The main disadvantages are: the large number of redundant data available in case it describes the behavior of a uniform soil, i.e. without variation in height; the need to change the density of the grating in order to describe the areas of increasing complexity; synonymous therefore of a lack of flexibility of the method, the direction of the sides of development of the grating goes towards privileged directions [Wack and Wimmer, 2002]. The grid structure can, therefore, be too approximate to effectively describe all the particular forms of the ground, but it is possible to increase the density of the grid and/or integrate the information with height measure of significant points.
The interpolation process can be defined as that mathematical algorithm which, starting from a set of points of coordinates (*x, y, z*) measured on a real surface, creates a new set of points in coincidence of a regular grid in *xy*, such that the surface defined by these is a representation as similar as possible to the surface to which the measured points belong. It must be considered that the interpolation algorithms have "anomalous" behavior in correspondence of the edges of the grid and that care must be taken to find the optimum pitch of the grid itself [Tanga et al., 2008; Kobler and Ogrinc, 2007].
In the TIN (Triangulated Irregular Network) model the elevation points are connected to these segments to form a continuous network of flat triangles, generally made with the algorithm of Delaunay in which the vertices (nodes) of the triangles are composed of the observed points. This avoids the problems of redundancy of information typical of the grid pattern and at the same time defines a DEM/DSM which is very effective in some modes of calculation.
Since the TIN constrained to pass through these points, tends to "recline" on the isolated points and along discontinuity lines and the profile, it thickens in correspondence of the areas where the density of the measured points is increased. The main advantages of this method are: the efficiency with which very irregular land can be modeled; the fitting of digital terrain model with these points, which represent the nodes of the triangles and thus act as "constraints"; the considerable reduction, with respect to the grid method, in the number of points that describe the surface [Peucker, 1978; Peucker et al., 1978; Kilian et al., 1996; Raber et al., 2002 a, b].
Many applications rely on accurate DTM. Suitable data are needed to create such models. Depending on the purpose digital representation and the size of the object, the data must meet various requirements, like acquisition of sufficient speed, high accuracy and acceptable cost. Since 1990 laser scanning technology characterized by high speed and good accuracy

has been introduced [Kolecka, 2011]. However, image-based methods have recently progressed. Especially in the field of information extraction from digital images. Many automatic algorithms have been implemented into different software, which effectively have improved and accelerated data processing [Kaartinen et al., 2005]. This is noninvasive and technologies prevent people from entering the areas surrounding the slope, that often leads to a serious danger. At the same time it provides digital documentation and gives a great potential for realistic and interactive visualization. The 3D modeling can be very efficient and useful when it comes to monitoring.

Empirical research in DEM accuracy assessment has observed that DEM errors are correlated with terrain morphology, sampling density, and interpolation method. The error variance and root mean squared error (RMSE), which are rooted in error propagation theory, have been widely applied [Tempfli, 1980; Li, 1993; Aguilar et al., 2006]. However, substantial challenges, both theoretical and practical, present to the applicability of these methods [Wise, 2000; Liu and Hu, 2007]. For example, while error propagation theory assumes that DEM errors are random and independent, many empirical studies have observed that DEM errors are actually correlated with terrain morphology and sampling density [Torlegard et al., 1986; Östman, 1987; Fisher, 1991; Hunter and Goodchild, 1995; Kyriakidis et al., 1999; Holmes et al., 2000; Lopez, 2002; Aguilar et al., 2005; Bonin and Rousseaux, 2005; Oksanen and Sarjakoski, 2006].

Peng Hu et al. [2009] have observed that DEM error is a combination of propagation error and interpolation error. When the source data has high vertical accuracy, propagation error is small, and therefore DEM error is dominated by interpolation error. In particular, from Table 1, it can be seen that interpolation error depends on two factors: $M_2$ or $M_4$ which are essentially descriptors of terrain morphology, and h which describes source data density because it measures the interval between two reference points.

**Table 1 - Error bound of three linear polynomial interpolations [Hu et al., 2009].**

| | $\delta_T$ random error propagation | $R_T$ interpolation error |
|---|---|---|
| Linear interpolation in 1D | $\lvert\delta_T\rvert \le \lvert\delta_{node}\rvert$ | $\lvert R_T\rvert \le 1/8 M_2 h^2$ |
| Tin interpolation | $\lvert\delta_T\rvert \le \lvert\delta_{node}\rvert$ | $\lvert R_T\rvert \le 3/8 M_2 h^2$ |
| Bilinear interpolation in a rectangle | $\lvert\delta_T\rvert \le \lvert\delta_{node}\rvert$ | $\lvert R_T\rvert \le 1/4 M_2 h^2 1/64 M_4 h^4$ |
| Total error | $\max\left(\lvert R_T\rvert + \lvert\delta_T\rvert\right) \le \max\lvert R_T\rvert + \max\lvert\delta_T\rvert$ | |

For a given study area, the value of $M_2$ or $M_4$ is fixed. If the terrain is very complex or source data are sparsely distributed, $M_2 \cdot h^2$ will be a large value. Under such circumstances, none of the interpolation methods in Table 1 will be effective.

However, interpolation error can still be reduced if the maximum interval h is decreased by inserting new reference points.

In the case that high density source data is available and the vertical accuracy of the source data is high, the interpolation error and the propagation error are both likely to be small. Consequently, any of the three interpolation methods in Table 1 is likely to result in an acceptable DEM. This is why interpolation method is less important when generating a DEM from LiDAR point data.

From Table 1, it can be seen that the propagation errors in the three linear polynomial methods are nearly the same. However, their interpolation errors vary significantly. Linear interpolation in 1D has much higher potential to result in a more accurate DEM

than the other two methods. This result is interesting considering that TIN is currently the dominant approach to interpolate a DEM. To explore the rigorous implementation of linear interpolation in 1D is thus a promising direction for future research on DEM generation.
The experimentation conducted in this study is aimed at designing and implementing an algorithm 1D designed to detect an automatic procedure for the generation of a DTM obtained by pseudo-regular grid with values of least squares shares compensated. It wanted to produce a DTM as close as possible to reality of the morphological soil detected, minimizing errors in the altimetric height determination [Huising et al., 1998]. The difference between the outputs of commercial software and of developed algorithm regards the interpolation method, in particular, the first is regular and has a grid size set by the operator, while the results of experimental algorithm is a pseudo-regular grid that may be increased and densified according to the precision requested. Moreover, the choice and selection of TLS points to be compensated is based on a iterative process conceptually clear, in which the compensation of the height points is made using the method of least squares.

## Area test

The object of the integrated survey, has been a dirt street located in the countryside of Martina Franca, a lovely town in the Itria Valley, located about 70 km from Bari and about 30 km from Taranto (Fig. 1). The street is connected through a coplanar with the state road 172, it connects the town of Itria Valley to Taranto.

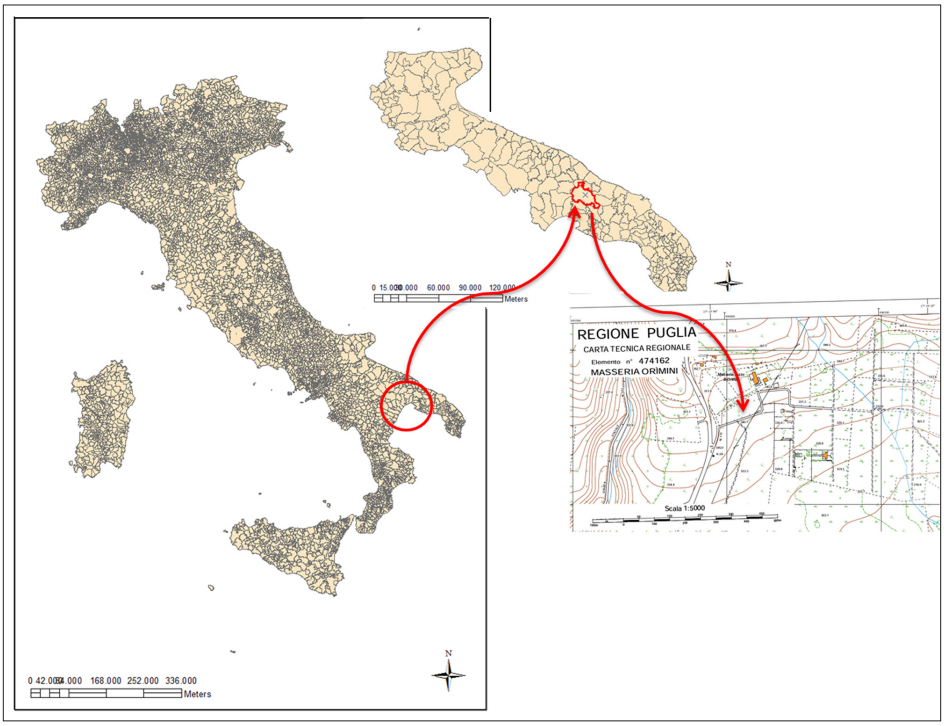


**Figure 1 - Study area location.**

The street is 105 meters long and 3 meters wide (Fig. 2). The choice has been dictated by the need to detect a street that was not a plan, but presented a change in elevation, with slopes in positive and negative variables without a regular trend, in order to highlight and enhance the quality of test results [Hyyppa and Yu, 2005].

**Figure 2 - Area Test.**

Also, an almost straight street has been chosen, in order to consider only a laser standpoint. The other characteristic of the surveyed street is the few and little vegetation, present only on the outer edges.

## Integrated survey

For the implementation of the integrated survey a total station Leica TPS1205 for the acquisition of topographic data and the Leica HDS3000 for TLS data has been used (Fig. 3). First, we performed the topographic survey in which, using a 360° reflective prism, 180 points properly distributed along the street have been collimated. The same points have been surveyed in RTK (Real Time Kinematic), but the results of this survey were used for subsequent elaborations since the accuracies were lower than those expected. The points have been taken for each cross section (at the middle and on both sides) in order to have the most uniform coverage possible and distant between 0.8 to 1 meters.

**Figure 3 - Field survey activities.**

The last step has been the laser survey, using the Leica HDS 3000, acquiring a scanning with a grid cell size 5×5 cm. The processing of the topographical data with LGO has provided the coordinates (*x,y,z*) in the local system.
The TLS data, have been georeferenced automatically by recording on the basis of three reflective targets, automatically recognized by the laser and topographically surveyed.
In particular, by acquiring with a semi-automatic procedure three target points suitably distributed on the street and previously surveyed by total station and, subsequently, starting the procedure of automatic alignment between two scanworlds: target topography survey and cloud point of the street. The whole process has been executed in the Cyclone proprietary software which has allowed to obtain a quick procedure with good results (the maximum RMS has been 0.001 m) [Lichti, 2004; Guarnieri et al., 2011].
The result is a georeferenced points cloud in the local frame of reference which, before proceeding with the trial, has been properly filtered to remove the vegetation on street sides and at the middle and lower parts, so the noise and the edge effects.
In particular, the processes of data filtering have been started through the proprietary software. The first step has been the advanced segmentation involving the use of multiple sub-selections to refine a selection (add or remove points) before segmentation, fitting, or other processes. After the initial selection, the viewpoint can be changed and a new fence can be drawn in order to make a more precise selection. The second step has been the

segmentation of a point cloud by distance from a point considered the maximum of local slope. The points within the indicated distance of the indicated point are now a separate point cloud that can be selected independently and therefore cancelled. Subsequently, the results has been refined with segmentation of a point cloud by intensity (Fig. 4).

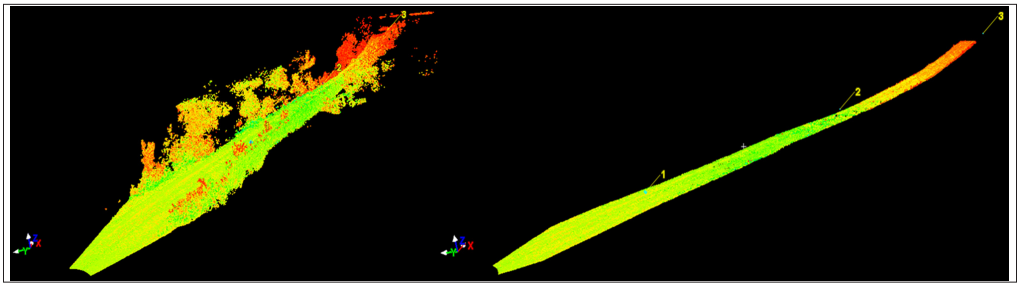

**Figure 4 - TLS point cloud pre and post filtering procedure.**

## DTM extraction with commercial software

### *DTM generation with StereoView*

StereoView enables the treatment of three-dimensional mathematical surfaces using the SV Dem model which is able to calculate the mathematical surface that best approximates the measured points.

The SV Dem is a module of StereoView Suite that allows, automatically, the interpolation of data points for the creation of digital terrain models, generation of contour lines, surfaces in triangular mesh or rectangular area. It serves to produce files that describe, using altitude information, the morphology of the territory, the quantity and goodness of the inserted points ensures the accuracy and robustness of the calculation. The possible functions are the following: DTM Digital Terrain Model and 3D MESH surface obtained by setting the parameters such as the horizontal and vertical step; 3D TIN surface; Convex Hull surface, and Contour Lines that allows to automatically generate contour lines. In the Interpolation Mode field it is possible to choose the cubic interpolation algorithm or BSPLINE. The choice depends on the data available. In each function of DEM "nodes" can be included (breaklines or breakpoints) which are lines or points of greatest weight in the computation order to improve the description of the terrain [Dequal et al., 1996].

In order to obtain the DTM (Fig. 5), the point cloud has been exported in ASCII format and it has been necessary to define the angle of orientation with respect to the x axis and the step of the grid both horizontally and vertically (expressed in unit of restitution) defined to 0.2 meters [Menci, 2000].

The use of StereoView has been dictated by the possibility to use a digital photogrammetric station at low cost yet able to perform automatic procedures using algorithms controlled.

### *DTM generation with Cyclone*

In Cyclone the DEM has been generated based on the georeferenced point cloud. The process includes the selection of the meshes to be sampled within a specific boundary, and also multi-selection of a polyline or polygon object. The samples have been taken

on the reference plane grid with determinated spacing. The output table check box has been selected to display the sample grid results dialogue that contains a table listing the individual sample points.

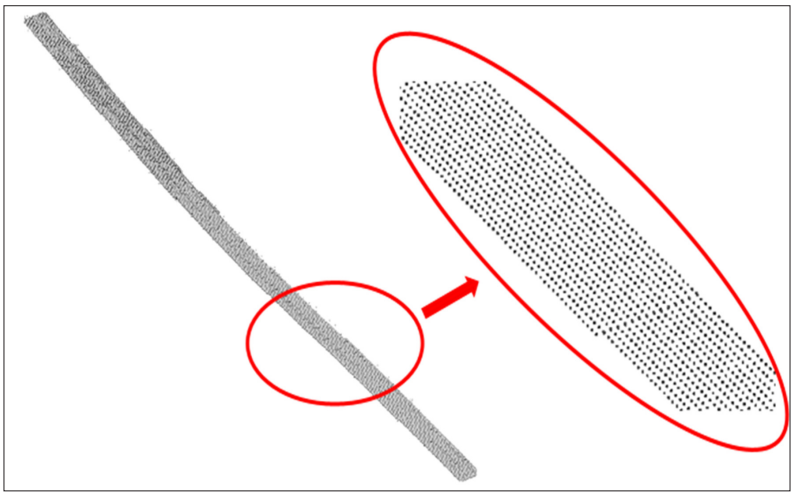

**Figure 5 - DTM in StereoView.**

In order to compare between Cyclone and StereoView results, in Cyclone the step interpolation grid of 0.2 meters has been adopted (Fig. 6) [Wack and Wimmer, 2002].

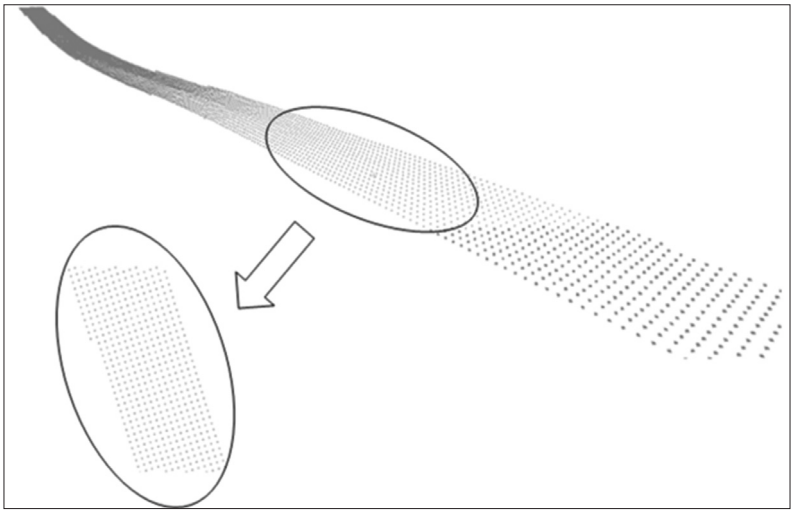

**Figure 6 - DTM in Cyclone.**

Cyclone has been used as a proprietary software of the instrument used.

## The results

The analysis of the results has been carried out by comparing the height of some sample points near the point of laser station in the center of the street and at the end of it, with respect to same points obtained for interpolation of two nearest neighbors TPS points.
The results have been evaluated for StereoView and plotted in a Cartesian graph (Fig. 7), in which $Q_{tps}$ and $Q_{intSV}$ indicate respectively the height determined with total station and the height obtained by interpolation in StereoView, the horizontal axis showing the distance in meters from the progressive point of laser station up to the last point (≈ 104 meters), and the vertical y-axis the deviation of height observed $\Delta Q$ in meters.

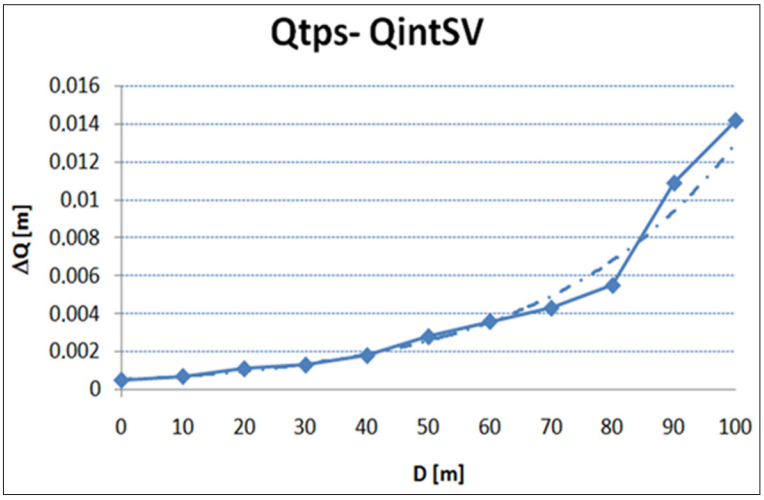


**Figure 7 - Comparision between TPS and StereoView data.**

What emerges is a direct proportionality between the distance $D$ from the station point $\Delta Q$, that is when the distance increases from the origin, of the local reference system, the deviation of the height is large, the latter increases exponentially from 80 meters, reaching values of 0.014 meters at the furthest point [Elberink et al., 2003]. This is due mainly to two factors: a) the accuracy of topographic survey (1 mm ± 1.5 ppm) that is much higher than that of the laser survey, b) the number of points surveyed by the HDS3000 is proportional to the scanning step and to the distance from the station point.
Even for the results of Cyclone, there is an increase of $\Delta Q$ with the distance $D$. However, deviation of 0.014 meters has been obtained in StereoView already about 75 meters by the station point down the street. The maximum deviation obtained at the maximum distance is 0.028 meters (Fig. 8, in which $Q_{intCyclone}$ indicate the height obtained by decimation in Cyclone).

## Experimental interpolation algorithm

The conceptual scheme of the experimental study is shown in Figure 9. It follows the description of the process used and the geometric algorithm.

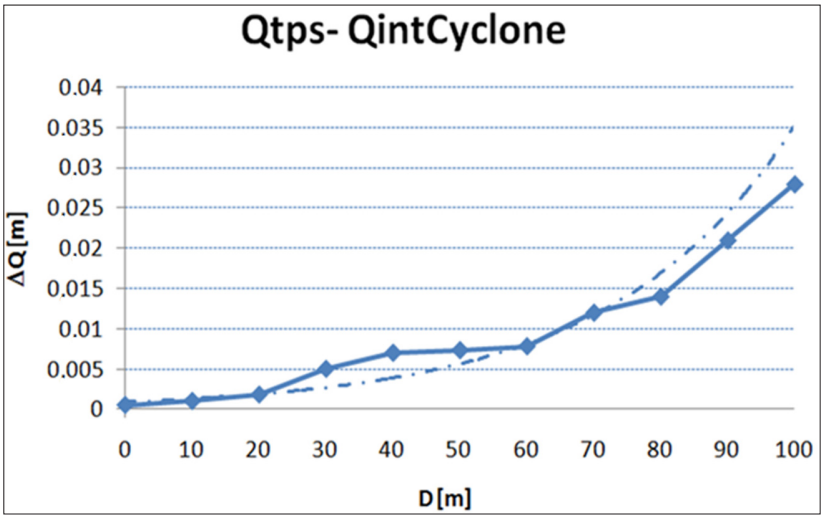


**Figure 8 - Comparison between TPS and Cyclone data.**

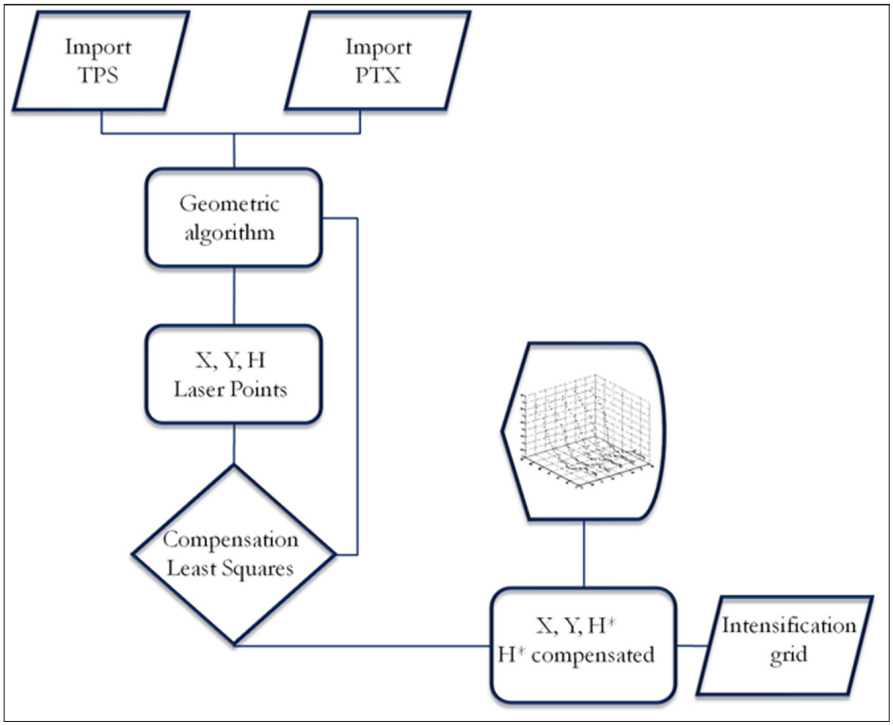


**Figure 9 - Conceptual framework of the methodology analyzed in the text.**

The determination of the points of the pseudo-regular grid is calculated by interpolation of the TLS points selected for subsequent steps from the 180 TPS points.

The advantage of this modus operandi regards both the "adaptive" ability of the grid in according to the density of the starting points and the base from which the calculations of compensation starts, [Axelsson, 1999, 2000] because this is always determined by known points topographically surveyed.
Being known the planimetric coordinates and the height of points topographically measured (TPS), it define the matrix of the vertices TPS as:

$$TPS = \begin{pmatrix} x_1 & y_1 & h_1 \\ \vdots & \vdots & \vdots \\ x_n & y_n & h_n \end{pmatrix} \quad n = 1,2,\cdots,180 \quad [1]$$

through which it is possible to calculate the position along $x$ ($H$, horizontal) and $y$ ($V$, vertical) of the respective midpoints ($M$):

$$M_{ij}^{h} = \begin{bmatrix} \frac{x_j + x_i}{2} \\ \frac{y_j + y_i}{2} \end{bmatrix} \quad \begin{matrix} i = 1,2,\cdots\cdots\cdots,n-1 \\ j = i+1 = 2,3,\cdots,n \end{matrix} \quad [2]$$

$$M_{ij}^{v} = \begin{bmatrix} \frac{x_j + x_i}{2} \\ \frac{y_j + y_i}{2} \end{bmatrix} \quad \begin{matrix} i = 1,2,\cdots\cdots\cdots,n-3 \\ j = i+3 = 4,5,\cdots,n \end{matrix} \quad [3]$$

Determined the above positions the laser point (LS) nearest to each of them is seeked, defined by the function of minimum distance:

$$\min\left[D_{TPS-LS}^{h}\right] = \begin{bmatrix} \sqrt{M_{ij}^{h} - P_1^{LS}} \\ \vdots \\ \sqrt{M_{ij}^{h} - P_k^{LS}} \end{bmatrix} \quad \begin{matrix} k = 1,2,3\cdots\cdots,m \quad and \\ m = number\ of\ laser\ point \end{matrix} \quad [4]$$

$$\min\left[D_{TPS-LS}^{v}\right] = \begin{bmatrix} \sqrt{M_{ij}^{v} - P_1^{LS}} \\ \vdots \\ \sqrt{M_{ij}^{v} - P_k^{LS}} \end{bmatrix} \quad \begin{matrix} k = 1,2,3\cdots\cdots,m \quad and \\ m = number\ of\ laser\ point \end{matrix} \quad [5]$$

The laser points $P_k^{LS}$ thus identified will constitute the DTM, and their increase will be defined at the execution of the different steps, respectively, in number equal to $k$:

$$k = \begin{cases} 2 + \left(\frac{n}{3} - 1\right) \times 5 & in\ 1^{st}\ step \\ \left(\frac{n}{3} - 1\right) \times 8 & in\ 2^{st}\ step \\ \left(\frac{n}{3} - 1\right) \times 14 - 4 & in\ 3^{st}\ step \\ \left(\frac{n}{3} - 2\right) \times 3 + 2 & in\ 4^{st}\ step \end{cases} \quad [6]$$

At each laser point is associated its relative height surveyed by TLS, which can be regarded as an approximate value for then, subsequently, an altimetric compensation to the indirect observations is performed, in the 1st step compared to the framework points (TPS) and so on of those of detail. The general equation is given by:

$$h_{p_k^{LS}} + h_{TPS_i} + h_{TPS_j} = v_k \quad [7]$$

For which given the system:

$$\begin{cases} AX + L = V \\ \sum_1^k p_k v_k = \min \end{cases} \quad [8]$$

that resolved will provide compensated height. Below parts of the listing in Matlab (Annex 1). From the TPS points, with the first step the network going to offset heights of 297 laser points has been increased (Fig. 10) selected among many on the basis of minimum distance from the midpoint between two adjacent TPS or rather $M_{12}$, $M_{23}$, $M_{27}$, etc.

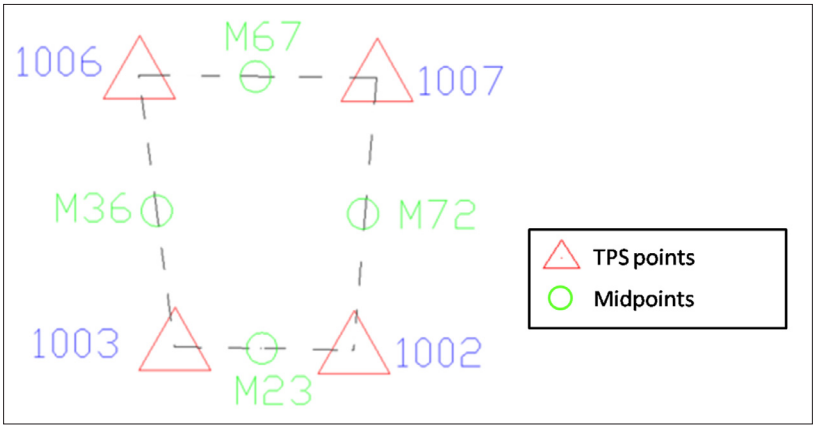


**Figure 10 - Principle of interpolation of the1th step.**

The TLS points closest to each midpoint calculated have been selected; subsequently, the height of the TLS selected points has been compensated by the method of least squares; finally compensated points, which have been assigned a sequential ID prefix 2000, and their coordinates have been exported into a new matrix called the SEL I (Fig. 11), which became the input file of the second iteration.

The SELI matrix obtained, the second follows, namely the identification and compensation of the additional 471 points. In this step, it is considered as starting grid, not that constituted by the TPS, but the one obtained in the previous step (SEL I).

The procedure adopted can be summarized as follows: the midpoints of all the points adjacent the SEL I have been calculated planimetrically (Fig. 12); the TLS points closer to the midpoints calculated have been identified and selected (Fig. 13).

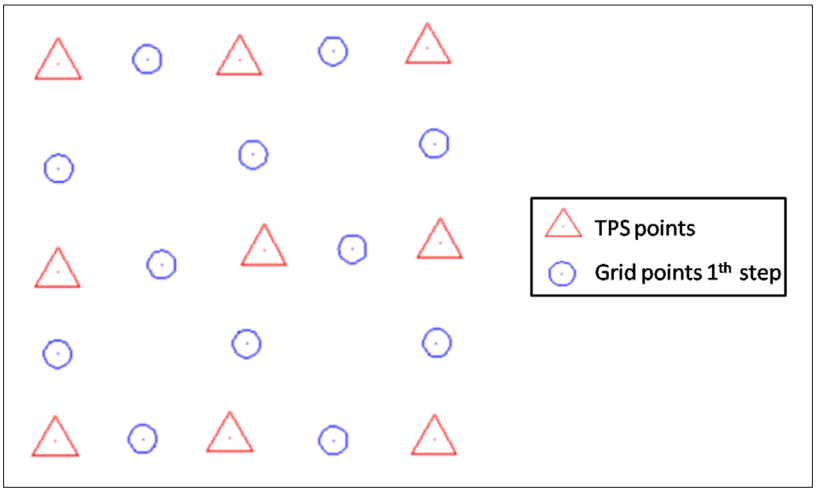


**Figure 11 - The detection of laser point for grid in the 1st step.**

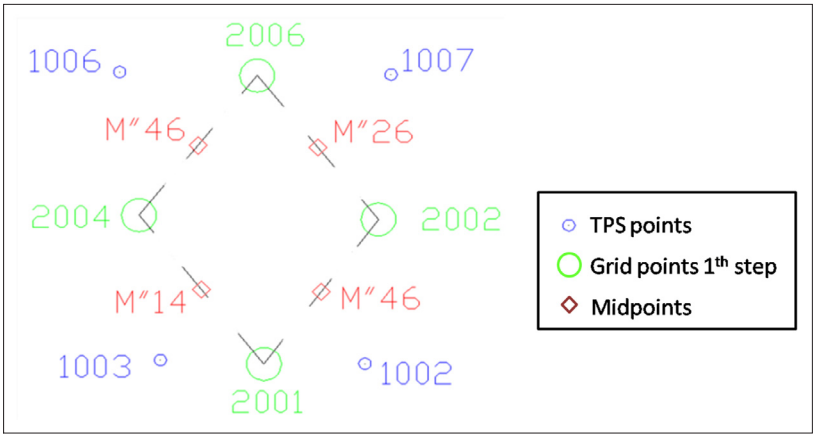


**Figure 12 - Principle of interpolation of the 2nd step.**

The height of selected laser points has been compensated with the method of least squares. To the compensated points and to their coordinates has been assigned a sequential ID code 3000 and have been saved in a new array, SEL II (Annex 2).
Subsequently, with the third step, the grid has been further thickened, identifying additional 821 compensated TLS points (Fig. 14) and selected with the same conceptual framework employed in the first step and taking as grid starting points those constituted by the points of SEL II. The interpolated data, which have been assigned a sequential ID code 4000, have been saved in a new matrix SEL III.
Subsequently, it has been carried out the last step (the fourth), with which the grid has been thickened with further 175 points (Fig. 15): the barycentre of quadrilaterals identified between more near points SEL III have been calculated planimetrically, taken at groups of four.

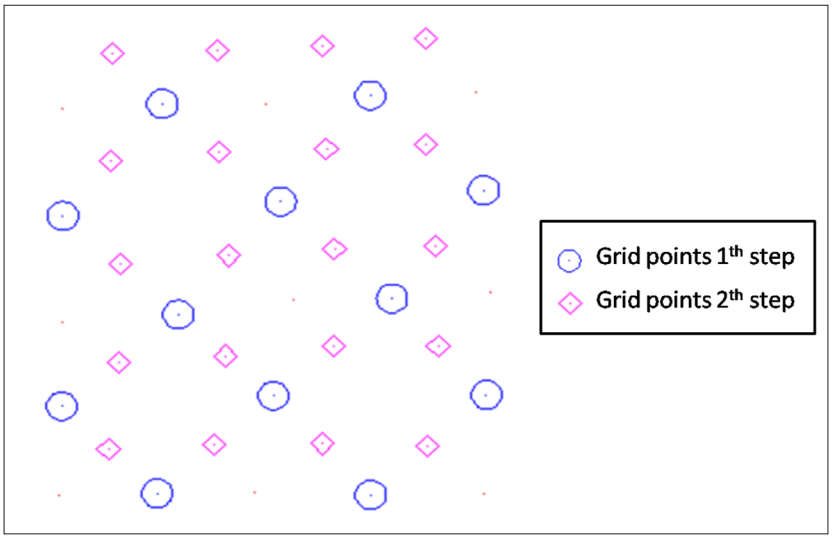


**Figure 13 - Grid points first and second step.**

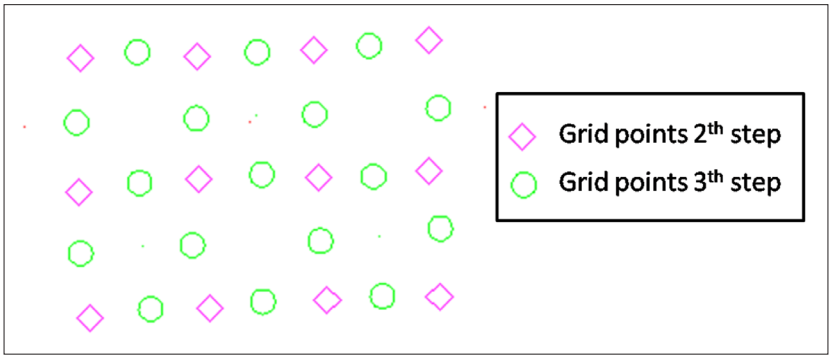


**Figure 14 - Grid points second and third step.**

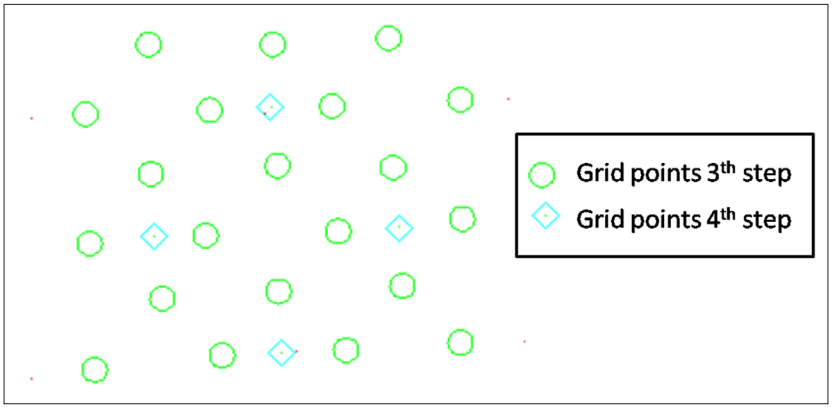


**Figure 15 - Grid points third and fourth step.**

TLS points closer to the calculated barycentric points calculated have been identified and selected, the height of the laser points selected. The compensated points, with sequential ID prefix 5000, have been inserted into a new array called SEL IV (Annex 3).
The interpolative process, which could be extended to the next step has been, however, stopped at the fourth step because of having reached a pitch of about 20 cm grid, that is comparable to the one set in the commercial software, to a reasonable and consistent comparison of the results [Gomes Pereira and Gonçalves, 2010].
In Figure 16 is shown a part of the interpolated and compensated grid obtained.

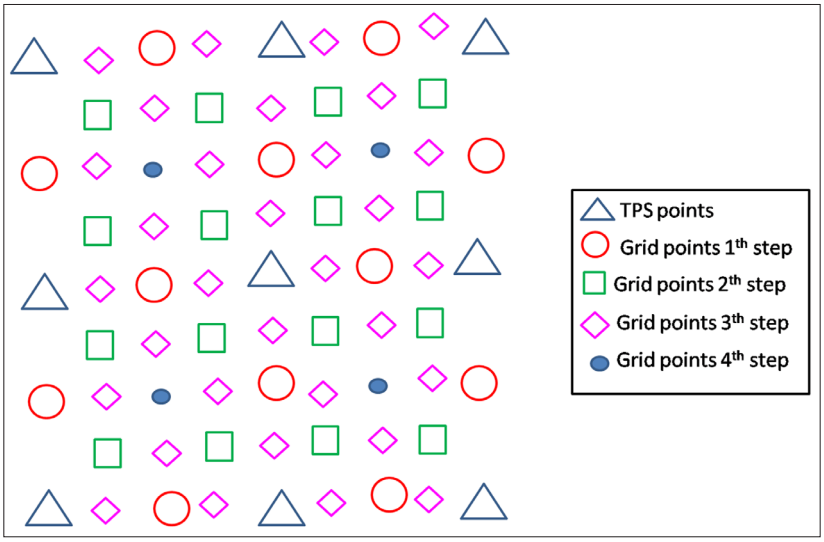


**Figure 16 - Overall view of the compensated points on a stretch of street.**

## Experimental results and discussion

The results obtained from each step have been exported to ASCII files and 3D images (Fig. 17). In particular, the matrices are composed of as many rows as interpolated and compensated points and four columns that denote the ID of the point, the $x$ coordinate, the $y$ coordinate and the compensated height $h$.
In Figure 18 the final result of the pseudo-regular grid, with the compensated height, with the visualization of the entire surface DTM is illustrated.
The DTM obtained by the experimental procedure and the output from both StereoView and Cyclone, have been exported in vector format and imported into AutoCAD with the application of "inspoints".
In order to analytically evaluate the result the difference in height (indicated by authors whit the symbol below) between the heights of the laser points surveyed ($Q$) and the height of the same after rigorous compensation ($Q_C$) with those between the laser height ($Q$) and the height of the points returned by StereoView ($Q_{SV}$) has been calculated.
In particular, for the results analysis points positioned in correspondence of the longitudinal axis of the street have been chosen. This, in order to, avoid any "edge effects" and therefore to make, the comparison more realistic.

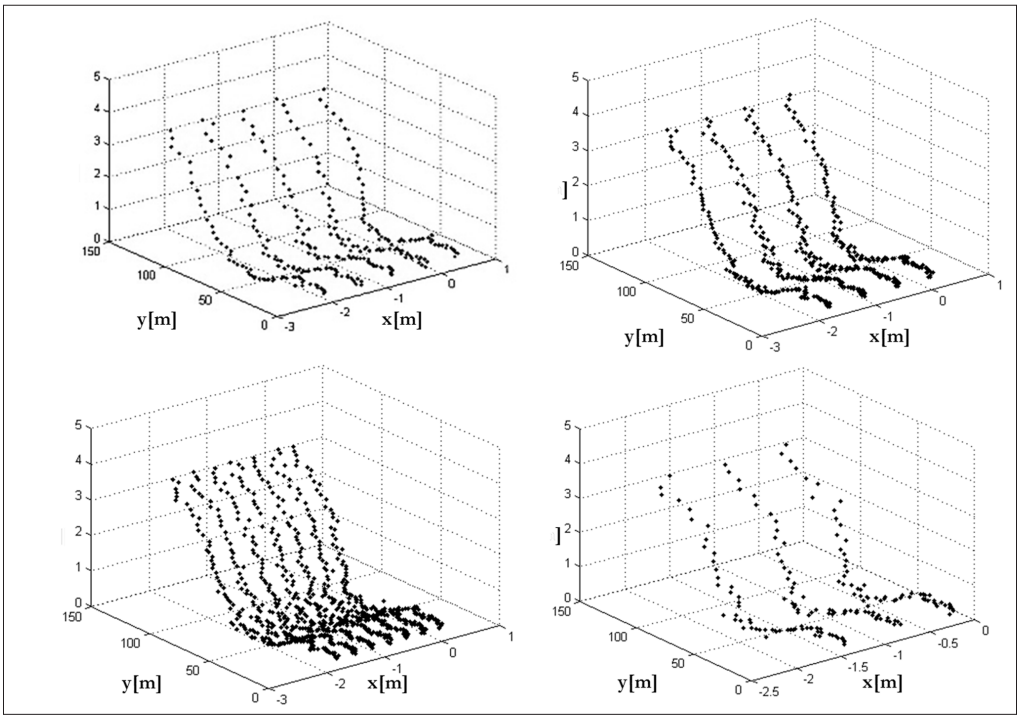


**Figure 17 - 3D visualization of the points found in local Cartesian system of different step.**

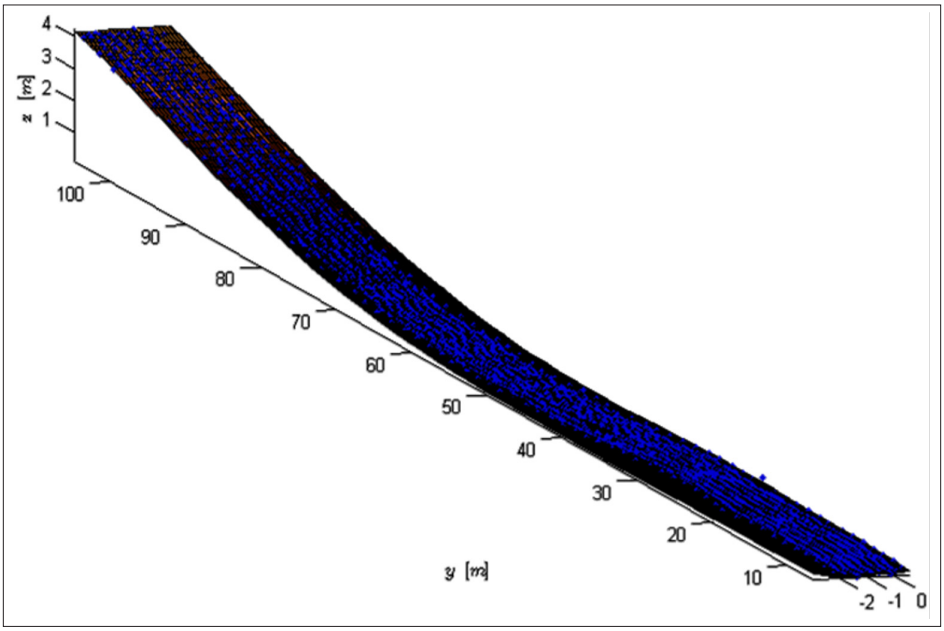


**Figure 18 - Visualization of the compensated DTM in 3D view.**

In fact, any criteria of interpolation adopted is unsuitable when it comes to describe the contours of the surface, for the obvious lack of measured points on one side (or rather two) of the study area. It often happens then to observe normal behavior of DTM at the edges of the grid, unless using complex algorithms or extending the area of which one wants the 3D model beyond the edges of the grid that you want to build in all direction. In this case study, since the implemented algorithm is aimed at the verification of the goodness of the method, it hasn't been necessary to reduce the "edge effects", obviously taken into account in the case of realization.
The obtained data are shown in Figure 19. The differences of height have a trend that increases with increasing distance from the station point.

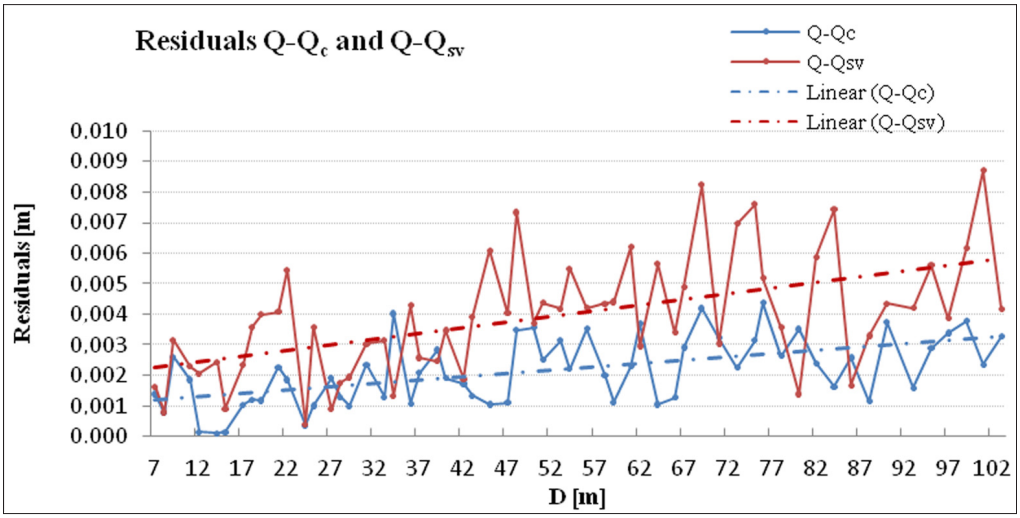


**Figure 19 - Diagram of residuals $Q$-$Q_c$ and $Q$-$Q_{sv}$.**

The values of ($Q$-$Q_c$) and ($Q$-$Q_{SV}$) tend to increase with the distance $D$ from the point of the station, while the residuals of ($Q$-$Q_{SV}$) are higher than those of ($Q$-$Q_c$), this to confirm that the DTM obtained in StereoView has been obtained for planimetric interpolation but not for the altimetric one and, therefore, it is of inferior quality. This demonstrates the effectiveness of the compensation process of the experimental algorithm, in fact, being the residuals ($Q$-$Q_c$) lower than ($Q$-$Q_{SV}$), it indicates that the obtained DTM has a altimetric trends more responsive to the reality respect the one obtained in StereoView, thus producing a reduction of errors in the determination of heights.
The maximum value of ($Q$-$Q_c$) is 4.5 mm and is equal to half the maximum deviation ($Q$-$Q_{SV}$) that is nearly 9 mm.
Following the same procedure of StereoView for Cyclone data ($Q_{cyc}$), the plotted have been obtained (Fig. 20), that allows direct comparison.
The residual ($Q$-$Q_c$) of the DTM experiment are even lower than those obtained with Cyclone. The differences, in fact, are most evident especially towards the end of the street where the maximum residual ($Q$-$Q_{cyc}$) exceeds one centimeter of difference.

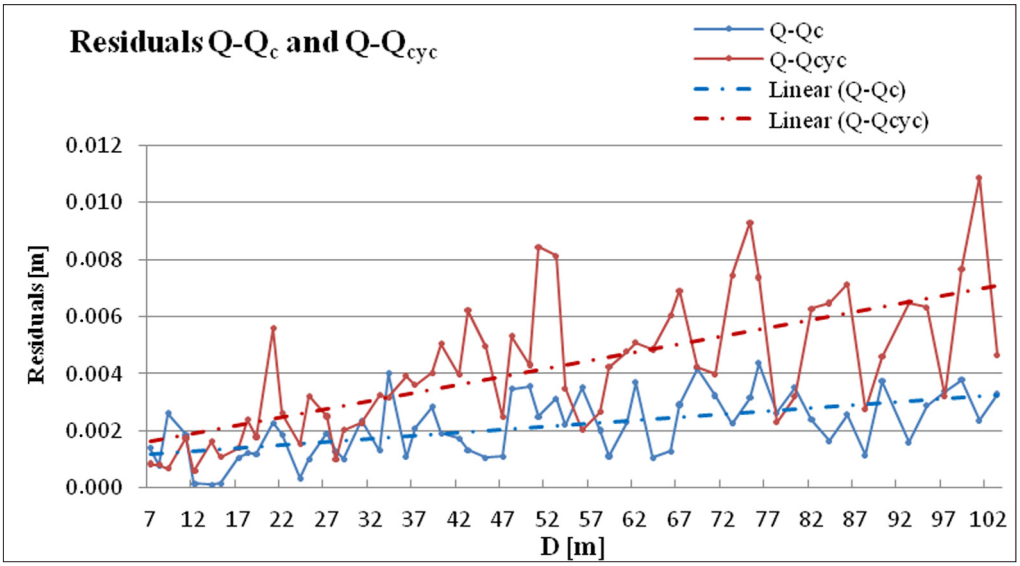


**Figure 20 - Diagram of residuals $Q$-$Q_c$ and $Q$-$Q_{cyc}$.**

## Conclusions

The experimental work has shown the ability to generate a DTM that is, as well as geometrically accurate, really altimetrical by using an automated algorithm, properly designed and implemented [Kraus and Pfeifer, 1998; Wack and Stelzl, 2005].

The results, though comparable to those that originate in the other two commercial software (StereoView and Cyclone), show the goodness of the procedure used.

In particular, experimental algorithm is able to contain the residuals of height in the acceptable limits (less than 4.5 mm) over a distance of 100 meters, to difference of StereoView that provided larger residuals (in our case up to 9 mm) and the Cyclone show edits lower reliability (height residual major at the centimeter) (Fig. 21).

The accuracy obtained at the end of this work is even comparable with that of the instrument of acquisition, while this is not possible to be said for the other two outputs where accuracy, while being tied to the instrument, decays much more quickly with distance, affecting the overall accuracy of the final result.

The algorithm developed while retaining the characteristics of ease application, is well suited to the description of any kind of surfaces thanks to the different conceptual organization that uses the principle of least squares of irregular grid. In addition, the procedure that allows the grid to be thickened, can be iterated almost "infinite" number of times in function of the need to represent the area with greater or lesser accuracy.

The strengths of the experimental study can be summarized mainly in:

- possibility to use the laser data for DTM with controllable height and the more accuracy;
- greater reduction of the survey time for the production of DTM of good quality;
- use of an integrated methodology easy to use;
- "adaptive" ability of the algorithm to the different needs of description of territory.

Moreover, this work will be improved by integrating the calculation procedure in a segmentation algorithm and filtering the data, by implementation and testing, necessary when we have to do with areas that have vegetation, as well for the production of "open source" software.

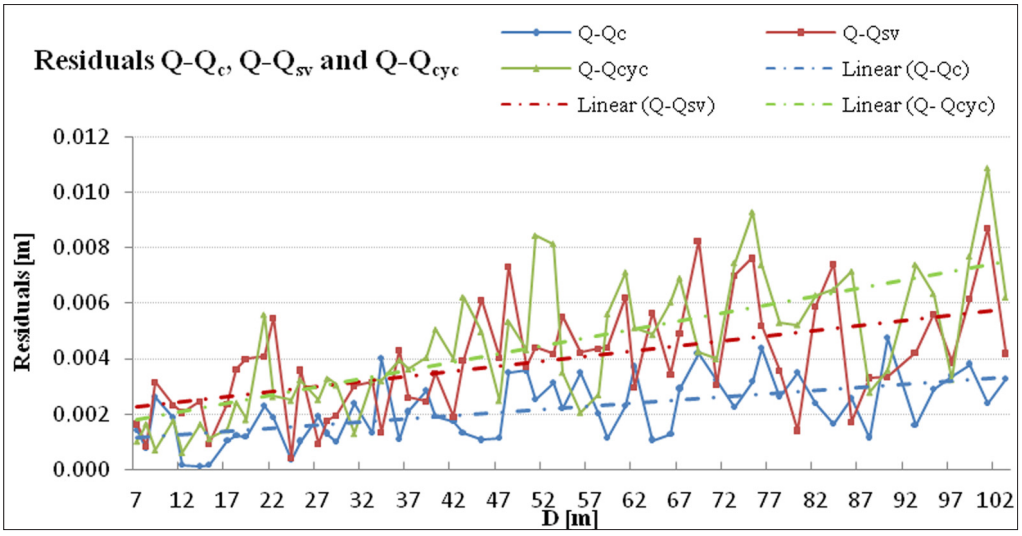


**Figure 21 - Diagram of residuals $Q$-$Q_c$, $Q$-$Q_{sv}$ and $Q$-$Q_{cyc}$.**

## Annex 1 – Algorithm 1. Selection of laser point and determination of its elevation, 1st step.

```
TPS=load('TPS.txt'); % Matrix of topographic points
TPS=TPS(:,1:4);
[m,n]=size(TPS);
a=0;
a=2+(m/3-1)*5;
med(a,3)=0;  % Matrix of midpoints first round
LAS=load('laser.txt'); % Matrix of laser points
[r,s]=size(LAS);
laser(a,4)=0;
SEL(a,4)=0; % Matrix laser points selected and compensated
d(4,r)=0;
app(4,1)=0;
% Calculationof coordinates of the midpoints between two points TPS
p=1;
i=1;
if p==1
    med(p,1)=2001;              % 1htmidpoint 1ht step
        med(p,2)=(TPS(i,2)+TPS(i+1,2))/2;
        med(p,3)=(TPS(i,3)+TPS(i+1,3))/2;
```

**Annex 1 (continued) – Algorithm 1. Selection of laser point and determination of its elevation, 1st step.**

```
for j=1:r
            d(1,j)=sqrt((med(p,2)-LAS(j,1))^2+(med(p,3)-LAS(j,2))^2);
            d(2,j)=LAS(j,1);
            d(3,j)=LAS(j,2);
            d(4,j)=LAS(j,3);
end
        app(1,1)=d(1,1);
        app(2,1)=d(2,1);
    app(3,1)=d(3,1);
        app(4,1)=d(4,1);
for j=2:r    % Selection of laser point nearest at midpoint p_i
if d(1,j)<app(1,1)
                app(1,1)=d(1,j);
                app(2,1)=d(2,j);
                app(3,1)=d(3,j);
                app(4,1)=d(4,j);
end
end
        SEL(p,1)=med(p,1);
        SEL(p,2)=app(2,1);
        SEL(p,3)=app(3,1);
        SEL(p,4)=app(4,1);
        laser(p,1)=med(p,1);
        laser(p,2)=SEL(p,2);
laser(p,3)=SEL(p,3);
        laser(p,4)=SEL(p,4);
% Rigorous compensation of elevation of selected laser points
……..
```

**Annex 2 – Algorithm 2, Selection of laser point and determination of its elevation, 2nd step.**

```
……
SELI=load('SELI.txt');
[p,q]=size(SELI);
% Calculationof coordinates of the midpoints between two points TPS (cfr.
Alg. 1)
……
SEL(u,1)=medII(u,1);
    SEL(u,2)=app(2,1);
    SEL(u,3)=app(3,1);
    SEL(u,4)=app(4,1);
    laser(u,1)=medII(u,1);
    laser(u,2)=SEL(u,2);
    laser(u,3)=SEL(u,3);
    laser(u,4)=SEL(u,4);
% Rigorous compensation of elevation of selected laser points
……
```

## Annex 3 – Algorithm 3, Selection of laser point and determination of its elevation, 3rd step.

```
……
SELIII=load('SELIII.txt');
SELIII=SELIII(:,1:4);
[h,k]=size(SELIII);
……
bar(z,3)=0;     % Matrix of barycentric points
……
z=1;
bar(z,1)=5001;
……
i=1;
    a1=sqrt(SELIII(i,2)-SELIII(i+1,2))^2+(SELIII(i,3)-SELIII(i+1,3))^2;
                 b=sqrt(SELIII(i+3,2)-SELIII(i+1,2))^2+(SELIII(i+3,3)-
SELIII(i+1,3))^2;
    c1=sqrt(SELIII(i+3,2)-SELIII(i,2))^2+(SELIII(i+3,3)-SELIII(i,3))^2;
                a2=sqrt(SELIII(i+7,2)-SELIII(i+1,2))^2+(SELIII(i+7,3)-
SELIII(i+1,3))^2;
                c2=sqrt(SELIII(i+3,2)-SELIII(i+7,2))^2+(SELIII(i+3,3)-
SELIII(i+7,3))^2;
p1=(a1+b+c1)/2;
    p2=(a2+b+c2)/2;
    s1=sqrt(p1*(p1-a1)*(p1-b)*(p1-c1));
    s2=sqrt(p2*(p2-a2)*(p2-b)*(p2-c2));
x1=(SELIII(i,2)+SELIII(i+1,2)+SELIII(i+3,2))/3;
    y1=(SELIII(i,3)+SELIII(i+1,3)+SELIII(i+3,3))/3;
    x2=(SELIII(i+1,2)+SELIII(i+3,2)+SELIII(i+7,2))/3;
y2=(SELIII(i+1,3)+SELIII(i+3,3)+SELIII(i+7,3))/3;
    bar(z,2)=(x1*s1+x2*s2)/(s1+s2);
    bar(z,3)=(y1*s1+y2*s2)/(s1+s2);
for j=1:r
        d(1,j)=sqrt((bar(z,2)-LAS(j,1))^2+(bar(z,3)-LAS(j,2))^2);
d(2,j)=LAS(j,1);
        d(3,j)=LAS(j,2);
        d(4,j)=LAS(j,3);
end
……
% Rigorous compensation of elevation of selected laser points
……
```

## References

Aguilar F.J., Aguera F., Agullar M., Carvajal F. (2005) - *Effects of terrain morphology, sampling density, and interpolation methods on grid DEM accuracy*. Photogrammetric Engineering & Remote Sensing, 71 (7): 805-816.

Aguilar F.J., Aguila M., Aguera F., Sanchez J. (2006) – *The accuracy of grid digital elevation models linearly constructed from scattered sample data*. International Journal of Geographical Information Science, 20 (2): 169-192. doi: http://dx.doi.org/10.1080/13658810500399670.

Axelsson P. (1999) - *Processing of laser scanner data - algorithms and applications*. ISPRS Journal of Photogrammetry and Remote Sensing 54 (2-3): 138-147. doi: http://dx.doi.

org/10.1016/S0924-2716(99)00008-8.

Axelsson P. (2000) - *DEM generation from laser scanner data using adaptive TIN models*. International Archives of Photogrammetry and Remote Sensing, XXXIII, Part B3, pp. 85-92, The Netherlands.

Bonin O., Rousseaux F. (2005) - *Digital terrain model computation from contour lines: How to derive quality information from artifact analysis*. GeoInformatica, 9 (3): 253-268. doi: http://dx.doi.org/10.1007/s10707-005-1284-2.

Dequal S., Lingua A., Rinaudo F. (1996) - *Matching techniques and algorithms for some basic photogrammetric procedures in the low cost digital photogrammetric system*. International Archives of Photogrammetry and Remote sensing, XXXII/5C1B, pp. 141-146.

Elberink S., Brand G., Brügelmann R. (2003) - *Quality improvement of laser altimetry DEM's*. Proceedings of the ISPRS workgroup III/3 workshop Dresden, pp. 71-78.

Fisher P.F. (1991) - *First experiments in viewshed uncertainty: The accuracy of the viewshed area*. Photogrammetric Engineering & Remote Sensing, 57 (12): 1321-1327.

Gomes Pereira L., Gonçalves G. (2010) - *Accuracy of a DTM Derived from Full-waveform Laser Scanning Data under Unstructured Eucalypt Forest: A Case Study*. FIG Congress 2010 Facing the Challenges – Building the Capacity. Sydney, Australia.

Guarnieri A., Vettore A., Camarda M., Costantino D. (2011) - *Automatic registration of large range datasets with spin-images*. Journal of Cultural Heritage, 12: 476-484. doi: http://dx.doi.org/10.1016/j.culher.2011.03.010.

Holmes K.O.A., Chadwick Kyriakidis P.C. (2000) - *Error in a USGS 30-meter digital elevation model and its impact on terrain modeling*. Journal of Hydrology, 233: 154-173.

Hu P., Liu X., Hu H. (2009) - *Accuracy Assessment of Digital Elevation Models based on Approximation Theory*. Photogrammetric Engineering & Remote Sensing, (75) 1: 49-56.

Huising E.J., Gomes Pereira L.M. (1998) - *Errors and accuracy estimates of laser data acquired by various laser scanning systems for topographic applications*. ISPRS Journal of Photogrammetry and Remote Sensing, 53 (5): 245-261. doi: http://dx.doi.org/10.1016/S0924-2716(98)00013-6.

Hunter G.J., Goodchild M.F. (1995) - *Dealing with error in spatial databases: A simple case study*. Photogrammetric Engineering & Remote Sensing, 61 (5): 529-537.

Hyyppa H., Yu, X., Hyyppa J., Kaartinen H., Honkavaara E., Ronnholm P. (2005) - *Factors affecting the quality of DTM generation in forested areas*. Proceedings of ISPRS Workshop on Laser Scanning 2005, (Netherlands: GITC bv), XXXVI, 3/W19, pp. 85-90. Enschede, The Netherlands.

Kaartinen H., Hyyppä J., Gülch E., Vosselman G., Hyyppä H., Matikainen L., Hofmann A.D., Mäder U., Persson Å., Söderman U., Elmqvist M., Ruiz A., Dragoja M., Flamanc D., Maillet G., Kersten T., Carl J., Hau R., Wild E., Frederiksen L., Holmgaard J., Vester K. (2005) - *Accuracy of 3D city models: EuroSDR comparison*. International Archives of Photogrammetry and Remote Sensing, vol. 36, 3/W19. The Netherlands: Enschede.

Kilian J., Haala N., Englich M. (1996) - C*apture and evaluation of airborne laser scanner data*. International Archives of Photogrammetry and Remote Sensing, vol. XXXI, B3, Vienna, Austria.

Kobler A., Ogrinc P. (2007) - *REIN Algorithm and the Influence of Point Cloud Density on NDSM and DEM Precision in a Submediterranean Forest*. ISPRS Workshop on Laser

Scanning 2007 and Silvi Laser 2007, Espoo, Finland.

Kolecka N. (2011) - *Photo-based 3D scanning vs. laser scanning – competitive data acquisition methods for digital terrain modelling of steep mountain slopes*. ISPRS Archives, XXXVIII-4/W19: 203-208.

Kraus K., Pfeifer N. (1998) - *Determination of terrain models in wooded areas with airborne laser scanner data*. ISPRS Journal of Photogrammetry and Remote Sensing, 53: 193-203. doi: http://dx.doi.org/10.1016/S0924-2716(98)00009-4.

Kyriakidis P.C., Shortridge A.M., Goodchild M.F. (1999) - *Geostatistics for conflation and accuracy assessment of digital elevation models*. International Journal of Geographical Information Science, 13: 677-707. doi: http://dx.doi.org/10.1080/136588199241067.

Li Z. (1993) - *Mathematical models of the accuracy of digital terrain model surfaces linearly constructed from square gridded data*. The Photogrammetric Record, 14 (82):661-674. doi: http://dx.doi.org/10.1111/j.1477-9730.1993.tb00776.x.

Lichti D. D. (2004) - *A Resolution Measure for Terrestrial Laser Scanners*. Proceedings of ISPRS XX Congress. Istanbul, Turkey, p. 6.

Liu X., Hu P. (2007) - *Accuracy assessment of digital elevation models based on approximation theory*. Proceedings of the Geographical Information Science Research UK Conference, Maynooth, Ireland (National Center for Geocomputation, National University of Ireland Maynooth), pp. 246-251.

Lopez C. (2002) - *An experiment on the elevation accuracy improvement of photogrammetrically derived DEM*. International Journal of Geographical Information Science, 16 (4): 361-375. doi: http://dx.doi.org/10.1080/13658810210129111.

Menci L. (2000) - *Stereospace: an idea for photogrammetric data collection*. International Archives of Photogrammetry and Remote Sensing, XXXIII (Part B2): 395-400.

Oksanen J., Sarjakoski T. (2006) - *Uncovering the statistical and spatial characteristics of fine toposcale DEM error*. International Journal of Geographical Information Science, 20 (4):345-369. doi: http://dx.doi.org/10.1080/13658810500433891.

Östman A. (1987) - *Accuracy estimation of digital elevation data banks*. Photogrammetric Engineering & Remote Sensing, 53 (4): 425-430.

Peucker T.K. (1978) - *Data Structures for Digital Terrain Models: Discussion and Comparison*. l[st] Int. Advanced Study Symposium on Topological Data Structures for Geographical Information Systems, Harvard Paper on Geographical Information Systems, Edited by G. Dutton, vol. 5.

Peucker T.K., Fowler R.J., Little J.J., Mark D.M. (1978) - *The Triangulated Irregular Network. American Society for Photogrammetry (ASP)*. ACSM Proceedings of Digital Terrain Models (DTM) Symposium, St. Louis, pp. 516-540.

Raber G.T., Jensen J.R., Schill S.R., Schuckman K. (2002a) - *Creation of digital terrain models using an adaptive Lidar vegetation point removal process*. Photogrammetry Engineering & Remote Sensing, 68 (12): 1307-1315.

Raber G.T., Hodgson M.E., Jensen J.R., Tullis J.A., Tullis Thompson G., Davis B., Schuckman K. (2002b) - *Comparison of LIDAR data collected leaf-on vs. leaf-off for the creation of digital elevation models*. Proceedings of the ASPRS 2002 Annual Convention, Washington, D. C. (American Society of Photogrammetry and Remote Sensing.

Tanga F.F., Liu J.N., Zhang X.H., Ruan Z.M. (2008) - *Derivation of digital terrain model in forested area with airborne lidar data.* The International Archives of the Photogrammetry,

Remote Sensing and Spatial Information Sciences, XXXVII (Part B3b): 343-348.
Tempfli K. (1980) - *Spectral analysis of terrain relief for the accuracy estimation of digital terrain models*. In: ITC Journal, 3: 478-510.
Torlegard K., Östman A., Lindgren R. (1986) - *A comparative test of photogrammetrically sampled digital elevation models*. Photogrammetria, 41:1-16. doi: http://dx.doi.org/10.1016/0031-8663(86)90002-5.
Wack R., Stelzl H. (2005) - *Laser DTM generation for South-Tyrol and 3D-visualization*. ISPRS WG III/3, III/4, V/3 Workshop "Laser scanning 2005", pp. 48-53. Enschede, the Netherlands.
Wack R., Wimmer A. (2002) - D*igital Terrain Models from Airborne Laser scanner Data – a Grid based approach*. Proceedings of the ISPRS Commission III Symposium Graz, pp. 293-296.
Wise S. (2000) - *Assessing the quality for hydrological applications of digital elevation of digital elevation models derived from contours.* Hydrological Processes, 14 (11-12): 1909-1929.

**Received 30/01/2012, accepted 15/01/2013**